SOME ASPECTS OF HARD-SCATTERING AT RHIC VERSUS THE COMBINATIONAL APPROACH

BHASKAR DE

Institute of Mathematical Sciences,
C.I.T. Campus, Taramani, Chennai-600113, India
bhaskar@imsc.res.in

S. BHATTACHARYYA*

Physics and Applied Mathematics Unit (PAMU),
Indian Statistical Institute, Kolkata-700108, India
bsubrata@isical.ac.in

The contrasting nature of the p_T-spectra measured in deuteron (D)–gold (Au) and gold (Au)–gold (Au) collisions, both performed at RHIC-BNL at $\sqrt{s_{NN}} = 200$ GeV, is now considered to be a very stimulating and hot topic in the domain of high energy nuclear physics. In continuation of our efforts to understand the measured data in high energy nuclear collisions in a somewhat nonstandard and alternative way, called the Combinational Approach (CA), we try here first to understand and reproduce the latest observations on deuteron–gold collisions at $\sqrt{s_{NN}} = 200$ GeV at mid-rapidity and some other rapidity regions with the same. Besides, (i) we also bring out the features of contrast for nuclear modification factor (NMF) in Au Au collisions at $\sqrt{s_{NN}} = 200$ GeV; (ii) for cross-checking of the present and previous results we also obtain the hadronic ratios measured for only the Au Au collisions at $\sqrt{s_{NN}} = 200$ GeV, as the data on the similar ratios for D Au interactions are not yet available. Finally, we point out the implications of the approach in terms of both data-interpretation and physical insights.

Keywords: Relativistic heavy ion collision, inclusive cross-section.

PACS numbers: 25.75.-q, 13.60.Hb

1. Introduction

In the most generalized manner, some of the most prominent experimental observations related to hard-scattering studies at RHIC are the following:[1] (i) The high-p_T yields of inclusive charged hadrons and π^0 in central Au Au at $\sqrt{s_{NN}} = 130$ and 200 GeV, are shown to be suppressed by as much as a factor 4–5 compared to PP

and peripheral Au Au yields scaled by some relevant physics factor; (ii) at intermediate p_T's ($p_T \simeq 2$–4 GeV/c) in central Au Au collisions, the measurements are at variance with the theoretical predictions for mesons, π^0 and K's. Furthermore, no suppression is seen for baryons yielding an "anomalous" baryon per meson ratio P/π^0 much larger than the perturbative $P/\pi \simeq 0.1$–0.3 ratio observed in PP collisions and e^+e^- reactions and (iii) high p_T productions probed in D Au reactions are not only not suppressed but it is enhanced compared to PP collisions, in a way very much analogous to the "Cronin Effect" observed in PA collision at lower center of mass energies. The second observation mentioned here has been taken care of by us in a separate work.[2] So, our thrust of the present work is on the first and third point mentioned above. Some other aspects of observations related to flow-behavior are here left out of the purview of the present work.

Obviously, the paramount importance on the observations of no suppression of the large-p_T hadrons in D Au reaction[3–6] for all the centrality ranges has been naturally pitted against the reported strong suppression in the central Au Au collisions[7,8] at the same $\sqrt{s}$-values. And this is projected as the signature of the quark–gluon plasma (QGP) physics in the standard vocabulary of present-day particle physics. Let us take a dispassionate view about any such description of physical phenomenon. In fact, in a series of recent works[9–12] we have quite elaborately analyzed a large body of the very recent results from both the CERN-SPS and BNL-RHIC in the light of a phenomenological model, called Combinational Approach (CA), which has no direct link with the QGP-tagged set of ideas. Rather in the plane of ideas, the CA essentially represents a unity of the Cronin-effect for nuclear collisions upto a critical value of p_T and a sort of the anti-Cronin-effect for the same beyond that limit, though structurally it is a combination of power-law form of fit for nucleon–nucleon (i.e. proton–proton) collisions and a parametrization by the present authors for the assumed nature of nuclear-dependence as would be evinced in the next section.

In the present paper we would try to interpret the measured data obtained from the RHIC-BNL experiments involving latest deuteron–gold collision at $\sqrt{s_{NN}} = 200$ GeV and some aspects of gold–gold collisions with the help of this same CA. And in the process we will not at all be concerned about whether the observed contrast is due to the "initial state effects" or "final state effects," as the controversy is now being broached about by the physicists. Our position and viewpoints are simple: nature manifests some physical realities in terms of the measured data on the various observables; and the task of any model/theory is to interpret them in a consistent way and with the number of assumptions and/or parameters as minimum as possible. The aim of this paper is to provide a successful and competent parametrization of the full ranges of the available data on the reported observables in D Au collisions at RHIC and on some aspects of Au Au collisions at RHIC.

In the next section we give a very brief sketch on the approach adopted here. The following section (Sec. 3) provides descriptions of the data analyses on D Au and Au Au interactions mostly in the graphical plots which technically represent some

of the most significant results based on this specific approach. The fourth section presents the results of our analyses of the hadronic ratios based on a previous work measured so far only for Au Au reactions. The last section offers the concluding remarks.

2. The Outline of the Combinational Approach

The expression for the transverse momentum-dependence of the inclusive cross-section for secondary particle, Q, produced in nucleus–nucleus (AB) collisions is given by:[9–12]

$$E\frac{d^3\sigma}{dp^3}\bigg|_{AB\to QX} \sim (AB)^{f(p_T)} E\frac{d^3\sigma}{dp^3}\bigg|_{PP\to QX}, \tag{1}$$

where A and B on the right-hand side of the above equation stand for the mass-numbers of two colliding nuclei; the term, $E\frac{d^3\sigma}{dp^3}|_{PP\to QX}$ is the inclusive cross-section for production of the same secondary, Q, in PP or $P\bar{P}$ collision at the same (center-of-mass) c.m. energy.

The nature of p_T-dependence of the inclusive cross-section term, $E\frac{d^3\sigma}{dp^3}|_{PP\to QX}$, occurring in Eq. (1), for production of a Q-species in $PP/P\bar{P}$ reactions at high energies is taken here in the form of a power-law as was initially suggested by G. Arnison *et al.*:[13]

$$E\frac{d^3\sigma}{dp^3}\bigg|_{PP\to QX} \approx C_1\left(1+\frac{p_T}{p_0}\right)^{-n}, \tag{2}$$

where C_1 is the normalization constant; and p_0 and n are two interaction-dependent parameters for which the values are to be obtained by fitting the PP and $P\bar{P}$ data at various energies. Of course, such a power-law form was applied to understand the nature of the tranverse momentum spectra of the pion secondaries by some other authors[14–17] as well.

Hence including Eq. (2) and a parametrization for the factor, $f(p_T)$, into Eq. (1), the final working formula is given by,[9–12]

$$E\frac{d^3\sigma}{dp^3}(AB\to QX) \approx C(AB)^{(\alpha p_T-\beta p_T^2)}\left(1+\frac{p_T}{p_0}\right)^{-n} \tag{3}$$

where C, α and β are constants and have to be determined by fitting the measured data on p_T-spectra for production of charged hadrons in nucleus–nucleus collisions at high energies. Some sort of physical interpretations for α and β are given in some of our previous works.[10,11]

A useful way[5,6] to compare the spectra from nucleus–nucleus collisions to those from nucleon–nucleon collisions is to scale the normalized PP (or $P\bar{P}$) spectrum (assuming the value of inelastic PP cross-section, $\sigma_{\rm inel}^{PP} \simeq 41$ mb) by the number of binary collisions, $\langle N_{\rm coll}\rangle$, corresponding to the centrality cuts applied to the

nucleus–nucleus spectra and construct the ratio. This ratio is called the nuclear modification factor (NMF), R_{AB}, which is to be expressed in the form

$$R_{AB} = \frac{\frac{1}{\langle N_{\rm coll}\rangle} E\frac{d^3N}{dp^3}\Big|_{AB}}{\frac{1}{\sigma_{\rm inel}^{PP}} E\frac{d^3\sigma}{dp^3}\Big|_{PP}} . \tag{4}$$

It is to be noted here that both the numerator and the denominator of equation (4) contain a term of the form $\left(1+\frac{p_T}{p_0}\right)^{-n}$ which gives the p_T-dependence of the hadronic-spectra produced in basic $PP/P\bar{P}$ collision. And as the other terms like, $\langle N_{\rm coll}\rangle$, $\sigma_{\rm inel}^{PP}$ are constants for a specific interaction at a definite energy and fixed centrality, we can obtain by combining Eqs. (3) and (4) the final expression for the ratio value in the following form:

$$R_{AB} \propto (AB)^{(\alpha p_T - \beta p_T^2)} . \tag{5}$$

The above steps provide the operational aspects of the combinational approach (CA). But, this combinational approach has the following few physical features: this outlines a method for arriving at the results to be obtained on some observables measured in particle–nucleus or nucleus–nucleus interactions at high energies from those obtained exclusively for only the basic nucleon–nucleon (or proton–proton) collision. And the results for nucleon–nucleon collisions are based on power-law form (Eq. (2)) which is supposed here to be fairly physically understood in the light of both thermal model and/or pQCD-related phenomenology. Besides, if the data sets on a specific observable are measured in PP reactions at five or six different high energies at reasonably distant intervals, the pure parameter-effects on p_0 and n could be considerably reduced and we may build up a methodology for arriving at p_0 and n values at any other different energy by drawing the graphical plots of p_0 versus $\sqrt{s}$ and n versus $\sqrt{s}$ curves, as are done in some of our previous works.[9,10] And on this supposition of availability of data in PP reactions at certain intervals of energy values, the number of arbitrary parameters for NA or AA collisions is reduced to only three which offer us quite a handy, useful and economical tool to understand the various aspects of the data characteristics.

3. Results

The p_0 and n values in Eq. (2) represent the contributions from basic NN (PP or $P\bar{P}$) collision at a particular energy. The values of p_0 and n are to be obtained from the expressions and plots shown in the work of De *et al.*[9,10] The relevant expressions are

$$p_0(\sqrt{s}) = a + \frac{b}{\sqrt{\frac{s_{NN}}{\rm GeV^2}}\ln\left(\sqrt{\frac{s_{NN}}{\rm GeV^2}}\right)} , \tag{6}$$

$$n(\sqrt{s}) = a' + \frac{b'}{\ln^2\left(\sqrt{\frac{s_{NN}}{\rm GeV^2}}\right)} . \tag{7}$$

Table 1. Values of a, b, a' and b' used in Eqs. (6) and (7) to obtain p_0 and n for various secondaries.

Secondary Type	a	b	a'	b'
$h^{\pm}$, $\pi^{0,\pm}$	1.5	79.4	6.5	127
$K^{\pm}$	1.6	103	3.6	161
P	7	602	5	644
$\bar{P}$	7	478	13	527

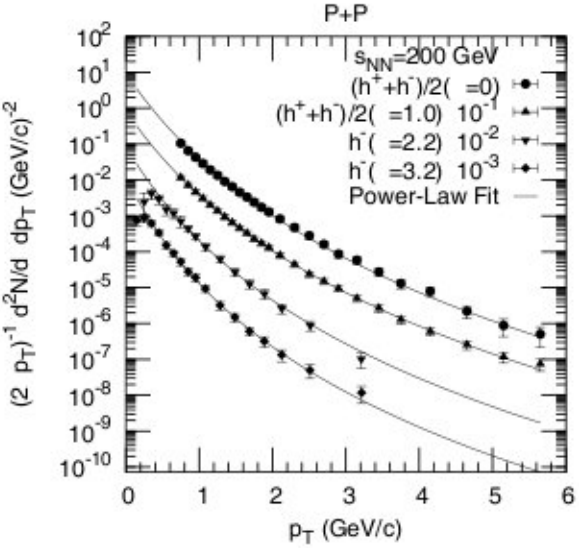

Fig. 1. Transverse momentum spectra for production of charged hadrons in PP collisions at RHIC energy in four different rapidity regions. The data are taken from Ref. 19. The solid curves represent the power-law-based fits (Eq. (2)).

The values of the parameters a, a', b and b' for different secondaries are given in Table 1. However, these values were obtained by analyzing the $PP/P\bar{P}$ data only in central rapidity region. In Fig. 1 we have shown the fit on the basis of power-law fit (Eq. (2)) to the invariant spectra of charged hadrons produced in RHIC PP collisions in the central rapidity region ($\eta = 0$), where the values of p_0 and n obtained from Eqs. (6) and (7) were supplied as inputs and the value of the normalization constant, C_1 was only fitted. But, the fits to the data in other rapidity regions have been obtained afresh in this work and these are shown in Fig. 1. Besides the values of different parameters are given in Table 2.

The fit values of α and β for secondary neutral pion produced in DAu reactions at $\sqrt{s_{NN}} = 200$ GeV in minimum bias events and those for charged hadrons produced in the same collision in minimum bias events and in four different centrality bins are given in Table 3. The fit results obtained on the basis of applications of these values for minimum bias and for various centralities of the collisions are

Table 2. Values of various parameters for production of secondary charged hadrons in PP collision at $\sqrt{s_{NN}} = 200$ GeV in different rapidity regions.

Secondary Type	C_1	p_0	n	χ^2/ndf
$(h^+ + h^-)/2$, $\eta = 1.0$	8.7 ± 0.9	1.51 ± 0.08	10.7 ± 0.2	0.065
h^-, $\eta = 2.2$	9 ± 1	1.27 ± 0.04	10.5 ± 0.2	1.205
h^-, $\eta = 3.2$	12 ± 2	1.05 ± 0.15	10.2 ± 0.7	0.151

Table 3. Values of different parameters for production of secondary charged hadrons and neutral pions in D Au collision at $\sqrt{s_{NN}} = 200$ GeV in central rapidity.

Secondary Type		C	α	β	χ^2/ndf
π^0	Min. Bias	31 ± 4	0.034 ± 0.008	0.0026 ± 0.0007	0.362
$(h^+ + h^-)/2$	Min. Bias	37 ± 2	0.075 ± 0.008	0.007 ± 0.001	0.610
	0–20% Central	39 ± 1	0.110 ± 0.005	0.013 ± 0.001	0.177
	20–40% Central	29 ± 1	0.104 ± 0.005	0.012 ± 0.001	0.128
	40–70% Central	20 ± 1	0.079 ± 0.007	0.010 ± 0.001	0.105
	70–100% Central	11 ± 1	0.057 ± 0.013	0.009 ± 0.002	0.124

Table 4. Values of various parameters for production of secondary charged hadrons in D Au collision at $\sqrt{s_{NN}} = 200$ GeV in different rapidity regions.

Secondary Type	C	α	β	χ^2/ndf
$(h^+ + h^-)/2$, $\eta = 0$	26 ± 1	0.117 ± 0.007	0.015 ± 0.001	0.112
$(h^+ + h^-)/2$, $\eta = 1.0$	26 ± 1	0.08 ± 0.01	0.011 ± 0.001	0.080
h^-, $\eta = 2.2$	24 ± 1	0.086 ± 0.007	0.011 ± 0.001	0.188
h^-, $\eta = 3.2$	18 ± 2	0.17 ± 0.03	0.06 ± 0.01	0.591

shown diagrammatically in Fig. 2. The Fig. 2(a) cites the model-based results by solid lines against minimum bias data on neutral pions and charged hadrons. And in Fig. 2(b) the same is presented for production of charged hadrons in four different centrality ranges of D Au reactions. These data are, in the main, obtained from the measurements done by PHENIX Collaboration.[3,5] In Fig. 3 the fits to the data from BRAHMS Collaboration[19] on charged hadron production in D Au collision at $\sqrt{s_{NN}} = 200$ GeV in different rapidity regions are shown. The values of α and β for these fits are given in Table 4.

The values of α and β, for central rapidity region ($\eta = 0$), worked here out phenomenologically are seen to be related to N_{part}, one of the very basic observables in heavy ion physics, which is called the number of participant nucleons in the nuclear collision. Another fundamental observable is the number of binary collisions (N_{coll}) which is also generally expressed in terms of N_{part} in the heavy ion literature. And both of them are the functions of the impact parameter. Very interestingly, long ago Giffon *et al.*[18] showed that the two dimensional impact parameter b is a conjugate variable to the two-dimensional transverse momentum (p_T) in much the

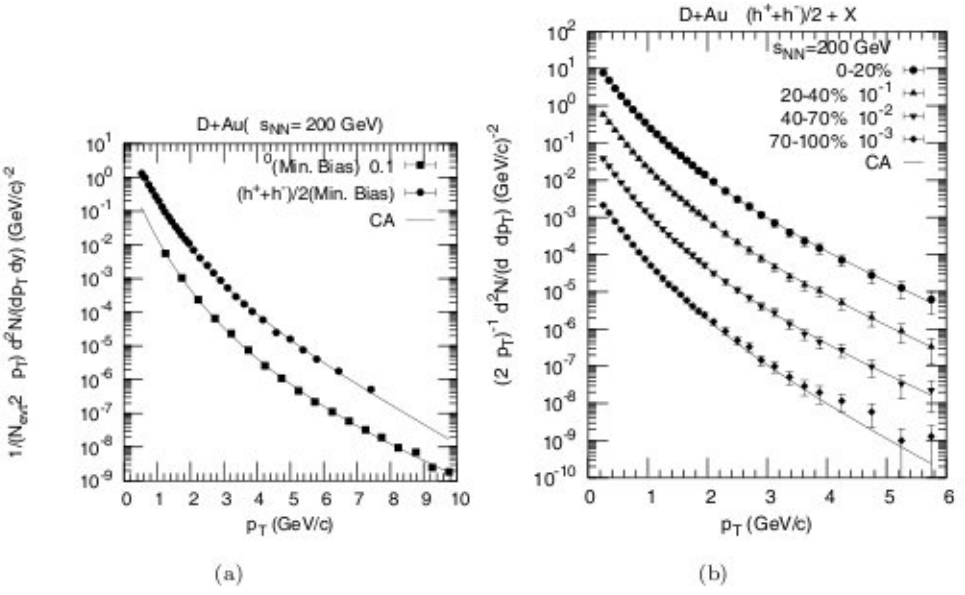

Fig. 2. Transverse momentum spectra for production of secondary charged hadrons and neutral pions in D Au collisions at $\sqrt{s_{NN}} = 200$ GeV for four centrality bins and in minimum bias events. The experimental data points are taken from Refs. 3 and 5. The solid curvilinear lines are drawn on the basis of combinational approach (CA).

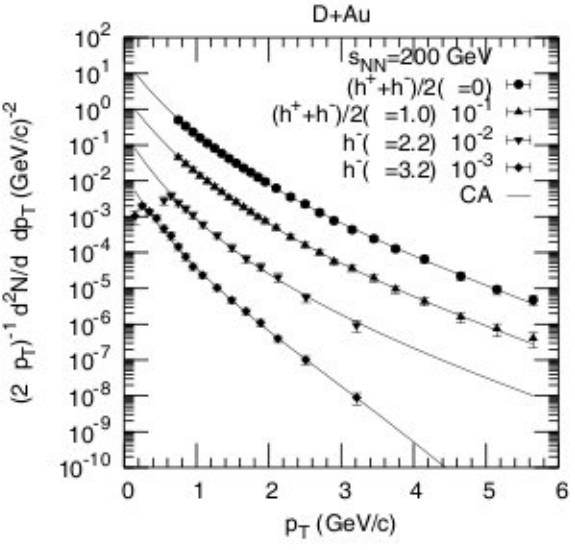

Fig. 3. Transverse momentum spectra for production of secondary charged hadrons in D Au collisions at $\sqrt{s_{NN}} = 200$ GeV for four rapidity-bins. The experimental data points are taken from Ref. 19. The solid curvilinear lines are drawn on the basis of Combinational Approach (CA).

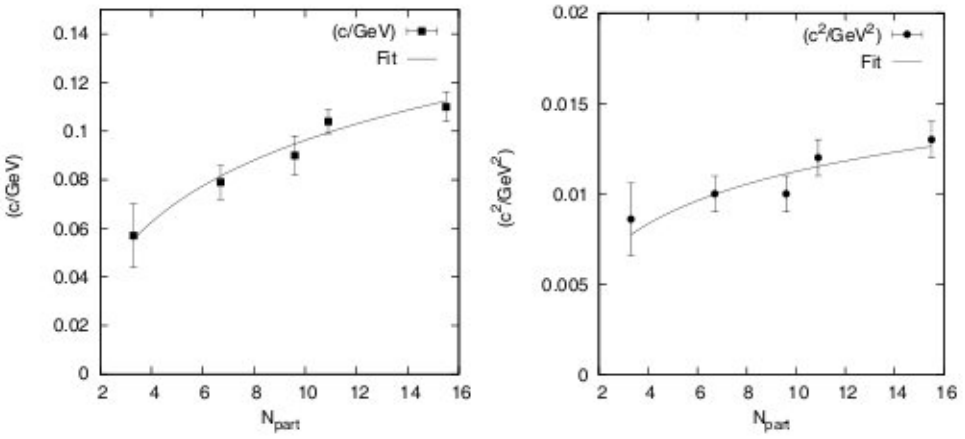

Fig. 4. Nature of centrality dependence of α and of β as functions of $N_{\rm part}$ for production of charged hadrons in D Au collision at $\sqrt{s_{NN}} = 200$ GeV. The data-looking points are here the parameter values taken from Table 1; and the solid curves give the two phenomenological fits as represented by the expressions in Eq. (8).

same way as position and momentum are conjugated variable operators in quantum mechanics since, the transition between the $b \Leftrightarrow p_T$ representations is obtained via a Fourier transform. They, thus, proposed a new sort of uncertainty relation between these two as $\Delta b \Delta p_T \simeq \hbar c$ or some close variant of it. However, with a view to accommodating the relationship with the physics of impact parameter we suggest the following two relations to describe the nature of the centrality dependence of the parameters α and β and they are depicted Fig. 4.

$$\begin{aligned} \alpha &= 0.011 + 0.037 \ln N_{\rm part} \,, \\ \beta &= 0.004 + 0.003 \ln N_{\rm part} \,. \end{aligned} \tag{8}$$

Figure 5(a) provides the model-based results computed from Eq. (5) and depicted by solid curves for production of neutral pions produced in D Au reactions in the minimum bias events and the Fig. 5(b) is the reproduction of the similar results for charged hadrons. The diagrams in Figs. 6(a)–6(d) portray the present model-based results by solid curves against those results obtained by PHOBOS Group[5] for the different centralities of the D Au collisions at $\sqrt{s_{NN}} = 200$ GeV. The theoretical uncertainty ranges arising out of the uncertainties in α and β are shown in both Figs. 5 and 6 by dashed curves. The results (presented in the diagrams of Figs. 5 and 6 as "data") are obtained from PHENIX[3] and PHOBOS[5] Collaborations who used a parametrization (Ref. 19 cited in Ref. 5) for $PP/P\bar{P}$-reaction data at $\sqrt{s_{NN}} = 200$ GeV. And this parametrization is somewhat different from that of ours here. The slight discrepancies between the "measured" and the computed values of $R_{\rm D\,Au}$ for the cases of minimum bias events with neutral pion and charged hadron production (Fig. 5) could be attributed to this source.

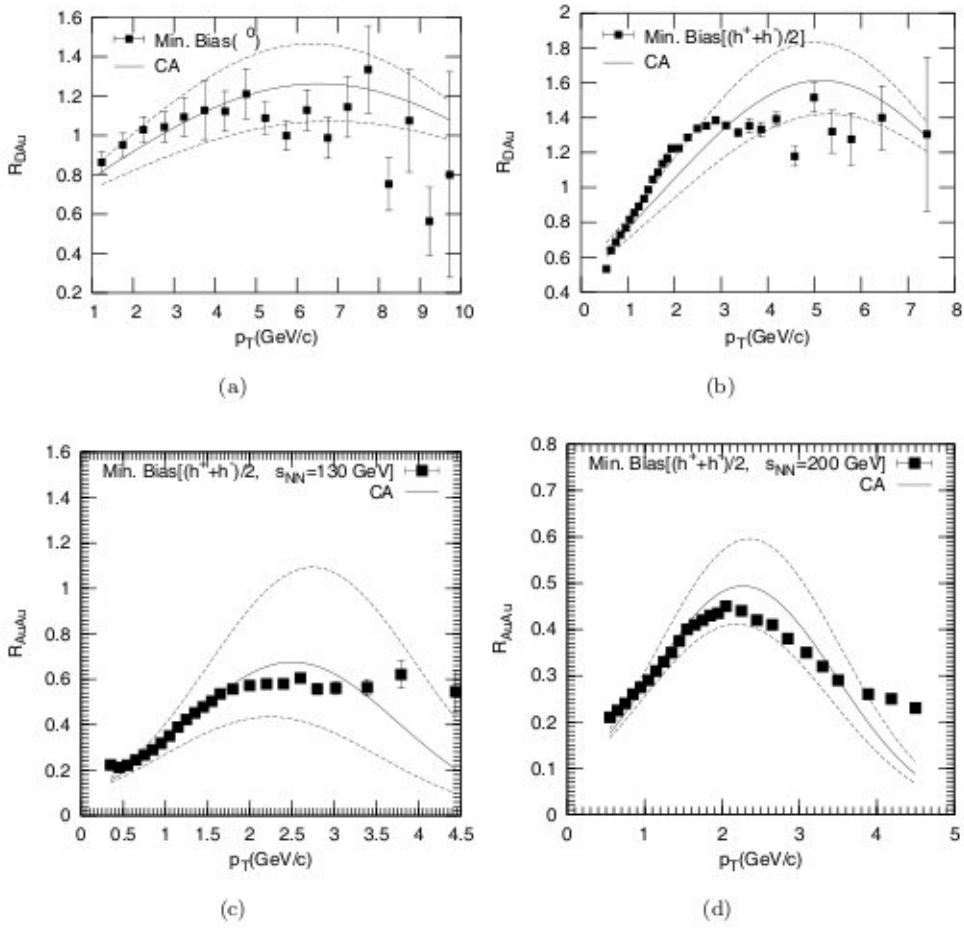

Fig. 5. Nature of Nuclear Modification Factor for production of neutral pions and charged hadrons in minimum bias D Au and Au Au collisions at RHIC energies as a function of p_T. The data-type points are taken from Refs. 3 and 20. The solid curves represent the results of CA and the dashed curves arise from the errors in α and β.

4. On Hadronic Ratios in Au Au Collisions

The essential purpose of this section is to provide a cross-checking of the results arrived at for both D Au and Au Au reactions. It is known that for D Au reaction measured data on separately identified charged hadrons are still not available; but they are at hand for Au Au interactions. Furthermore, data on some ratio behavior in Au Au interactions are also obtained. So, in the present work we propose to take up the studies on the nature of the various ratio-behaviors. And in so doing we are forced to revise a part of our previous work, as the present ratios are based on more uptodate and corrected data. In Figs. 8 and 9 we offer the renewed fits which slightly alter the parameters reported previously by us.[12] Tables 5–11 present the

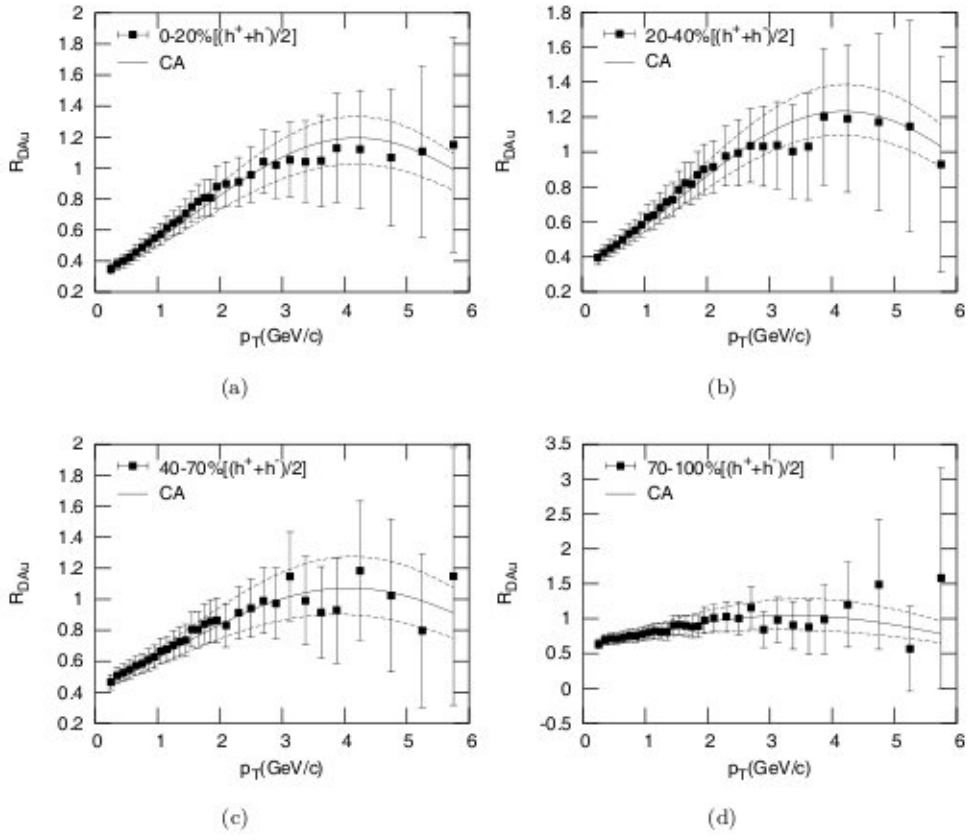

Fig. 6. Nature of p_T-dependences of R_{DAu} for production of charged hadrons in D Au collisions at RHIC energy in four centrality-bins. The data-type points are taken from Ref. 5. The solid curves represent the results of CA and the dashed curves arise from the errors in α and β.

corrected sets of the parameter values, and all the ratios are worked out on the basis of these updated parameter values. The solid curves drawn in the plots of Figs. 10–15 depict the nature of the ratios obtained by CA against data sets.

5. Concluding Remarks

By both the visual standards and the criteria of the χ^2/ndf values, if and wherever they are available, the nature of agreement between the measured data and the model-based results on the observables is, in most cases, modestly satisfactory. And this performance rating is obtained by a methodology which has nothing to do with the standard concepts extant in the domain of heavy ion literature. Evidently, the method employed involves use of a parametrization of experimental data in terms of the existing knowledge available from the analyses of simple $PP/P\bar{P}$ reaction at high energies. This leads to obtain a sort of universal description of the heavy ion collisions at high energies and to explain the available data on Au Au and

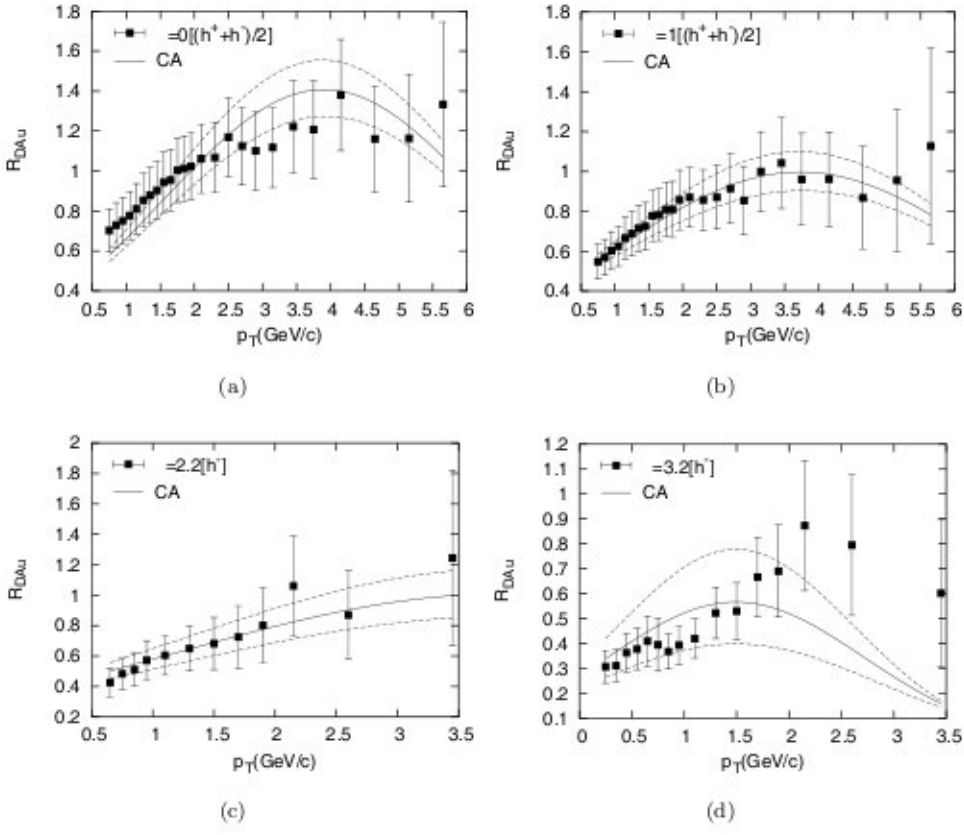

Fig. 7. Nature of p_T-dependences of $R_{\mathrm{D\,Au}}$ for production of charged hadrons in D Au collisions at RHIC energy in four rapidity regions. The data-type points are taken from Ref. 19. The solid curves represent the results of CA and the dashed curves arise from the errors in α and β.

D Au interactions with the help of a few parameters. The net outcome is: with this approach we have explained the signs of strong suppression in Au Au reaction at $\sqrt{s_{NN}} = 200$ GeV as is shown in the plots of Figs. 5(c) and 5(d). Furthermore, with the same approach we also explain here what is considered as the absence of suppression in D Au reaction. So, the data on both the reactions are understood and explained, irrespective of whether there is suppression or no suppression. The agreements are obtained not only for the cases of the data sets on the three or four inclusive p_T-spectra of the detected neutral pions, or hadrons in general, but also for the nuclear modification factors, R_{AB} as defined in the text by expression (4) with the same values of α and β at specific centralities indicated in the diagrams and depicted by the Tables 3 and 4. Obviously, such broad agreements cannot just be fortuitous, though we fail to readily respond to the questions in very concrete terms why and how the model works as a physical formalism with an underlying dynamics.

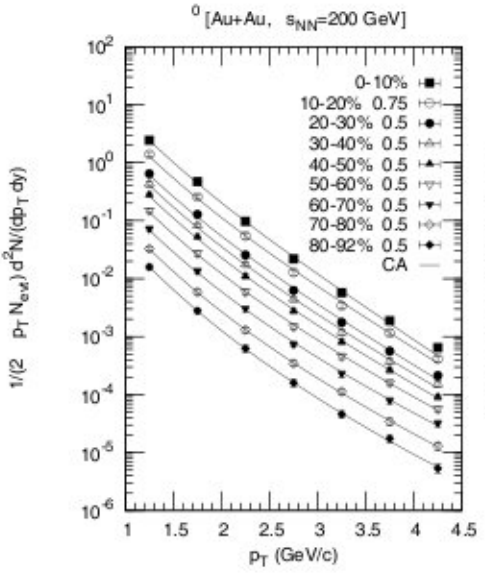

(a)

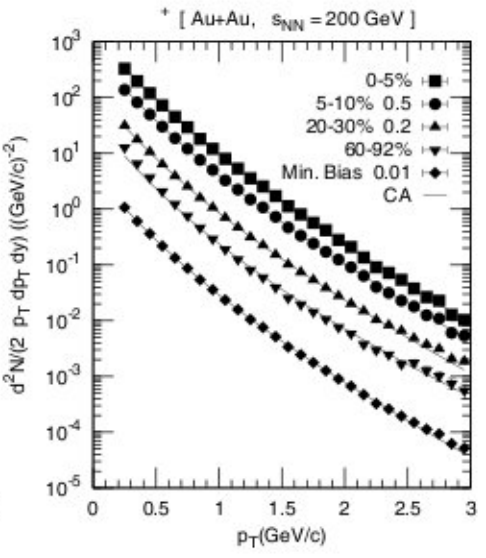

(b)

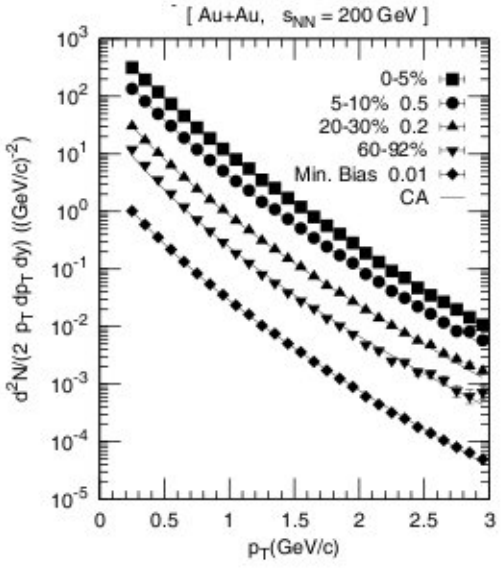

(c)

Fig. 8. Nature of transverse momentum spectra for secondary neutral and charged pions produced in Au Au collisions at $\sqrt{s_{NN}} = 200$ GeV at different centralities. The experimental data have been taken from Refs. 8 and 21. The solid lines depict the CA-based results on the basis of Eq. (3).

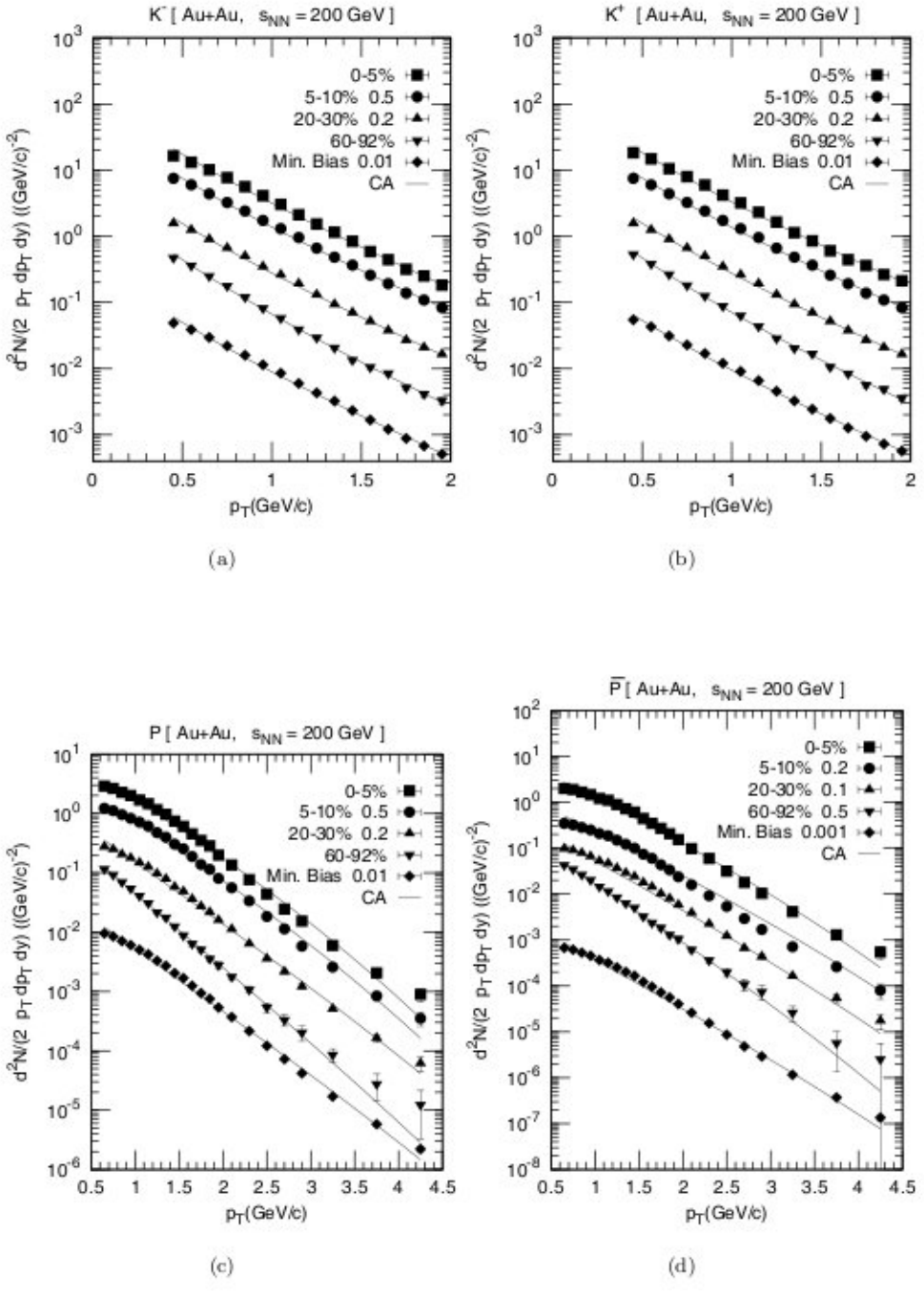

Fig. 9. Plots of invariant spectra of secondary charged kaons, protons and antiprotons produced in Au Au collisions at $\sqrt{s_{NN}} = 200$ for various centrality-bins. The experimental data points are taken from Ref. 21. The solid curves provide the CA-based fits.

Table 5. Parameter values for production of secondary neutral pions in Au Au collision at $\sqrt{s_{NN}} = 200$ GeV.

Centrality	C	α(c/GeV)	β(c/GeV)^2	χ^2/ndf
0–10%	888 ± 54	0.070 ± 0.003	0.016 ± 0.001	0.510
10–20%	619 ± 50	0.068 ± 0.002	0.013 ± 0.001	1.048
20–30%	455 ± 33	0.065 ± 0.002	0.012 ± 0.001	0.883
30–40%	322 ± 22	0.058 ± 0.005	0.011 ± 0.001	0.731
40–50%	219 ± 9	0.054 ± 0.003	0.010 ± 0.001	0.273
50–60%	118 ± 6	0.050 ± 0.003	0.008 ± 0.001	0.377
60–70%	61 ± 3	0.043 ± 0.004	0.006 ± 0.001	0.400
70–80%	31 ± 1	0.036 ± 0.002	0.0053 ± 0.0005	0.072
80–92%	17 ± 3	0.027 ± 0.008	0.004 ± 0.002	0.153

Table 6. Parameter values for production of secondary π^+ in Au Au collision at $\sqrt{s_{NN}} = 200$ GeV.

Centrality	C	α(c/GeV)	β(c/GeV)^2	χ^2/ndf
0–5%	1565 ± 31	0.066 ± 0.002	0.024 ± 0.001	0.232
5–10%	1301 ± 53	0.064 ± 0.006	0.021 ± 0.002	0.311
20–30%	702 ± 6	0.058 ± 0.001	0.017 ± 0.002	2.168
60–92%	45 ± 3	0.041 ± 0.004	0.011 ± 0.001	1.969
Min. Bias	482 ± 3	0.058 ± 0.001	0.018 ± 0.003	1.318

Table 7. Parameter values for production of secondary π^- in Au Au collision at $\sqrt{s_{NN}} = 200$ GeV.

Centrality	C	α(c/GeV)	β(c/GeV)^2	χ^2/ndf
0–5%	1565 ± 31	0.066 ± 0.002	0.024 ± 0.001	0.220
5–10%	1301 ± 64	0.065 ± 0.007	0.022 ± 0.002	0.438
20–30%	691 ± 4	0.059 ± 0.001	0.017 ± 0.002	1.061
60–92%	44 ± 2	0.039 ± 0.003	0.010 ± 0.001	1.810
Min. Bias	465 ± 7	0.058 ± 0.001	0.017 ± 0.003	0.263

Table 8. Parameter values for production of secondary K^+ in Au Au collision at $\sqrt{s_{NN}} = 200$ GeV.

Centrality	C	α(c/GeV)	β(c/GeV)^2	χ^2/ndf
0–5%	150 ± 6	0.081 ± 0.003	0.025 ± 0.002	0.737
5–10%	124 ± 5	0.080 ± 0.002	0.025 ± 0.002	0.728
20–30%	65 ± 2	0.077 ± 0.002	0.025 ± 0.002	0.685
60–92%	4.8 ± 0.2	0.038 ± 0.003	0.019 ± 0.002	0.369
Min. Bias	44 ± 2	0.079 ± 0.003	0.025 ± 0.002	0.595

Table 9. Parameter values for production of secondary K^- in Au Au collision at $\sqrt{s_{NN}} = 200$ GeV.

Centrality	C	α(c/GeV)	β(c/GeV)^2	χ^2/ndf
0–5%	136 ± 3	0.092 ± 0.008	0.030 ± 0.005	0.977
5–10%	118 ± 4	0.090 ± 0.002	0.029 ± 0.002	0.608
20–30%	63 ± 2	0.085 ± 0.002	0.029 ± 0.002	0.598
60–92%	4.4 ± 0.1	0.040 ± 0.001	0.021 ± 0.001	0.474
Min. Bias	40 ± 1	0.085 ± 0.001	0.028 ± 0.002	0.776

Table 10. Parameter values for production of secondary protons in Au Au collision at $\sqrt{s_{NN}} = 200$ GeV.

Centrality	C	α(c/GeV)	β(c/GeV)^2	χ^2/ndf
0–5%	12.7 ± 0.9	0.18 ± 0.01	0.030 ± 0.001	1.175
5–10%	11.4 ± 0.7	0.175 ± 0.002	0.028 ± 0.001	1.644
20-30%	9 ± 1	0.14 ± 0.01	0.019 ± 0.003	1.409
60-92%	0.82 ± 0.06	0.09 ± 0.01	0.019 ± 0.004	0.621
Min. Bias	6.0 ± 0.9	0.13 ± 0.02	0.019 ± 0.004	1.615

Table 11. Parameter values for production of secondary antiprotons in Au Au collision at $\sqrt{s_{NN}} = 200$ GeV.

Centrality	C	α(c/GeV)	β(c/GeV)^2	χ^2/ndf
0–5%	11 ± 2	0.21 ± 0.02	0.029 ± 0.005	1.616
5–10%	10 ± 2	0.19 ± 0.02	0.025 ± 0.005	1.314
20–30%	6 ± 1	0.17 ± 0.02	0.023 ± 0.004	1.157
60–92%	0.55 ± 0.04	0.14 ± 0.01	0.027 ± 0.004	0.488
Min. Bias	4.2 ± 0.7	0.17 ± 0.02	0.022 ± 0.004	1.244

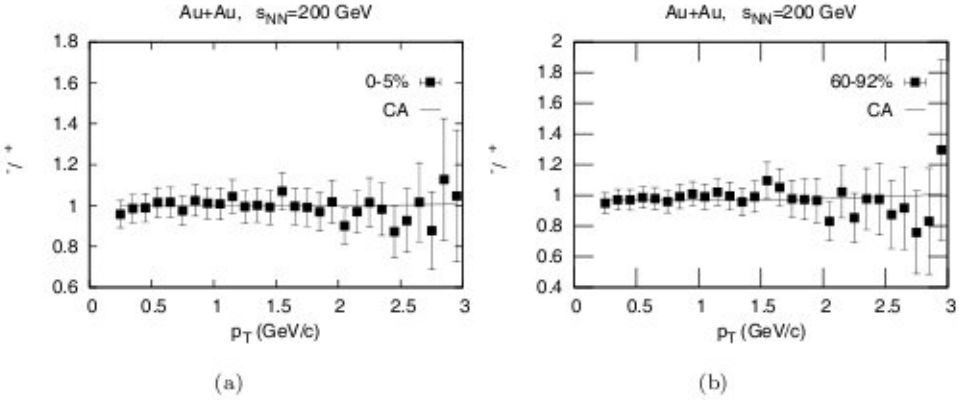

Fig. 10. Particle ratios of π^-/π^+ and K^-/K^+ for central and peripheral Au Au collisions at $\sqrt{s_{NN}} = 200$ GeV. The measured data are taken from Ref. 21. The solid lines provide the CA-based results.

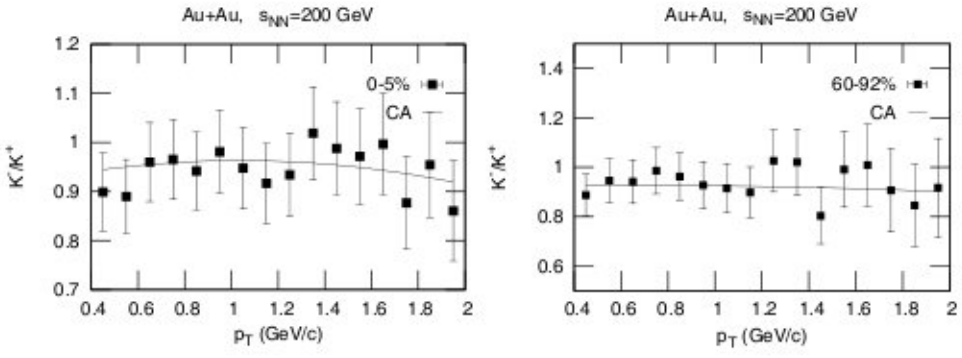

(c) (d)

Fig. 10 (*Continued*)

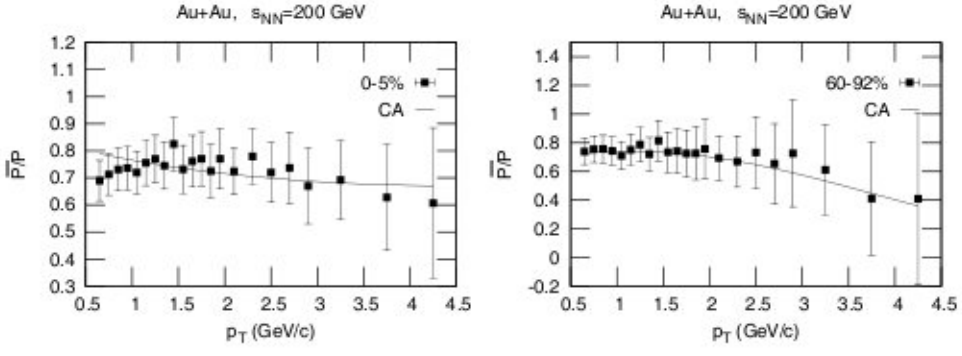

(a) (b)

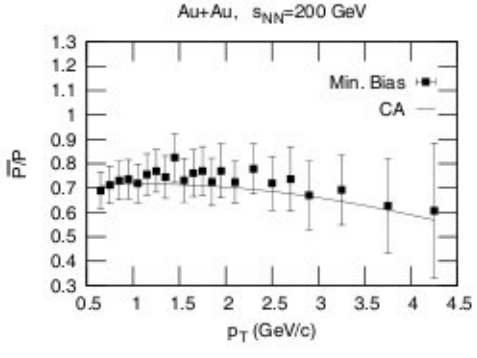

(c)

Fig. 11. $\bar{P}/P$ ratios as a funtion of p_T at central, peripheral and minimum bias Au Au collisions at $\sqrt{s_{NN}} = 200$ GeV. The experimental data are taken from Ref. 21. The solid lines provide the CA-based results.

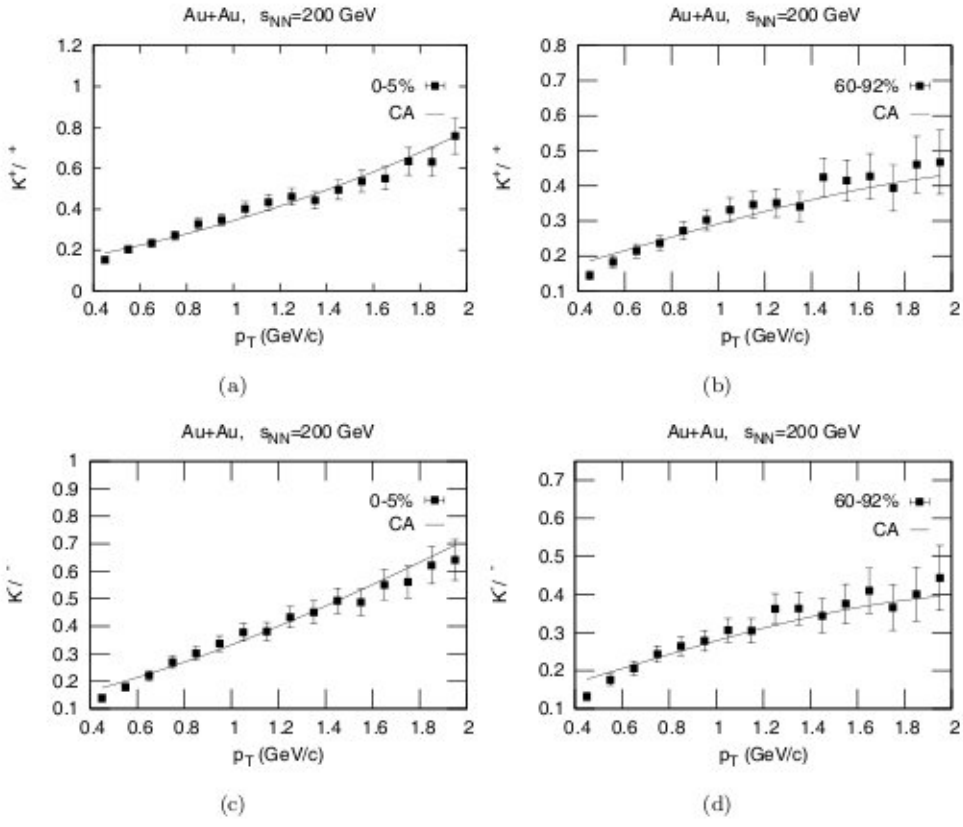

Fig. 12. Nature of transverse momentum dependence of K/π ratios at central and peripheral Au Au collisions at $\sqrt{s_{NN}} = 200$ GeV. The experimental data are taken from Ref. 21. The solid lines are drawn on the basis of the present work (CA).

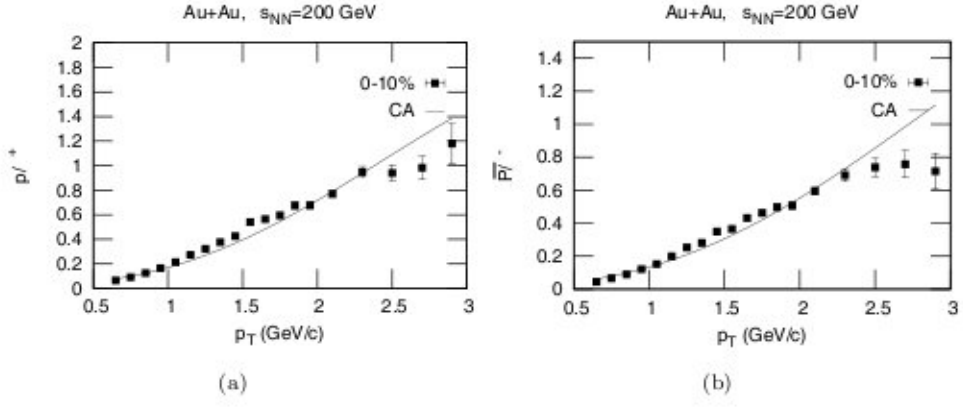

Fig. 13. p_T dependence of P/π^+ and $\bar{P}/\pi^-$ ratios at three different centra Au Au collisions at $\sqrt{s_{NN}} = 200$ GeV. The experimental data are taken from Ref. 21. The solid lines are drawn on the basis of the present work (CA).

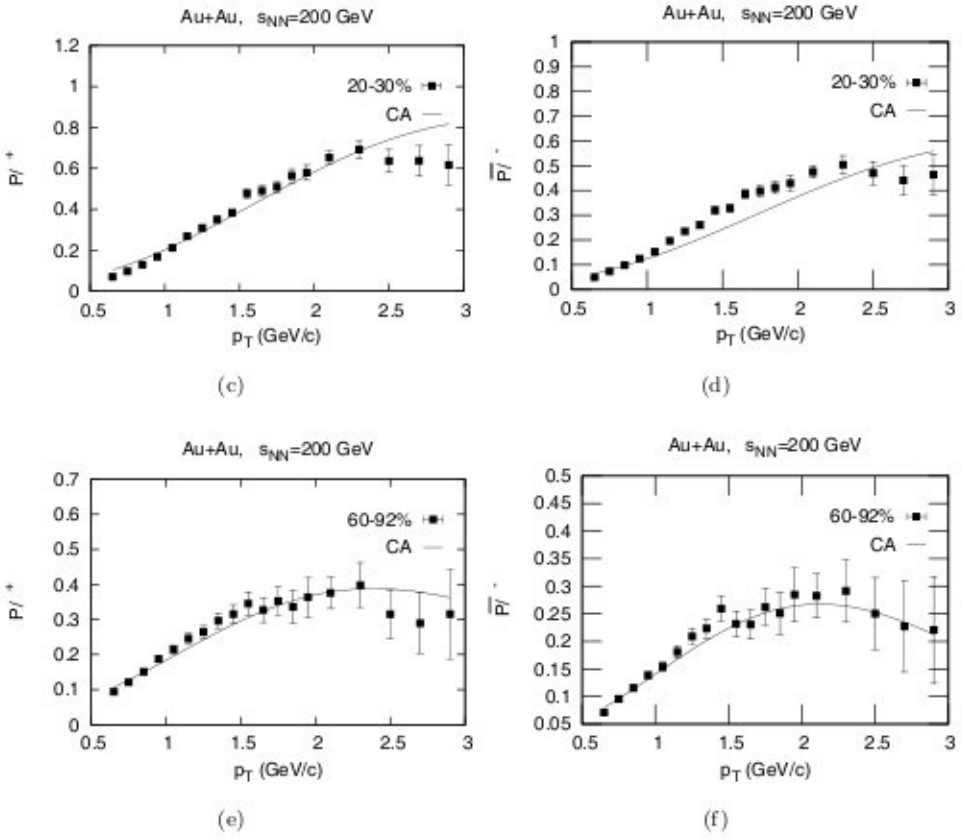

Fig. 13 (*Continued*)

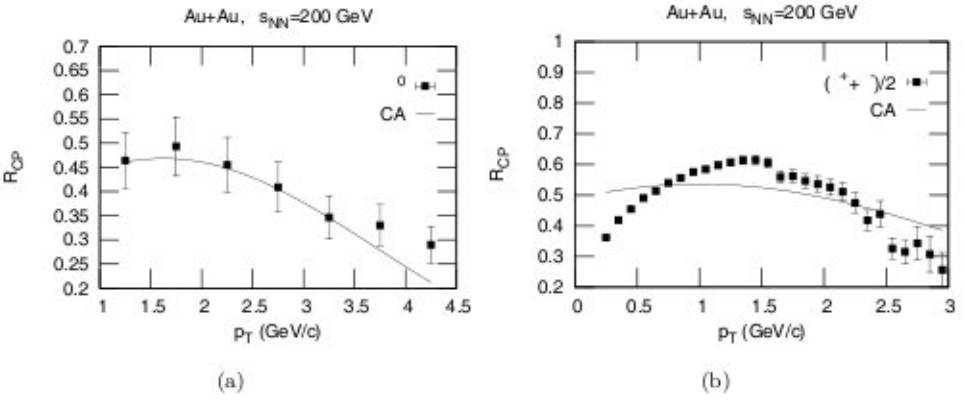

Fig. 14. Central (0–10%) to peripheral (60–92%) ratios of binary-collision-scaled p_T-spectra, R_{cp}, for pions, kaons and protons produced in Au Au collision at $\sqrt{s_{NN}} = 200$ GeV. The data points are taken from Ref. 21. The CA-based results are shown by solid curves.

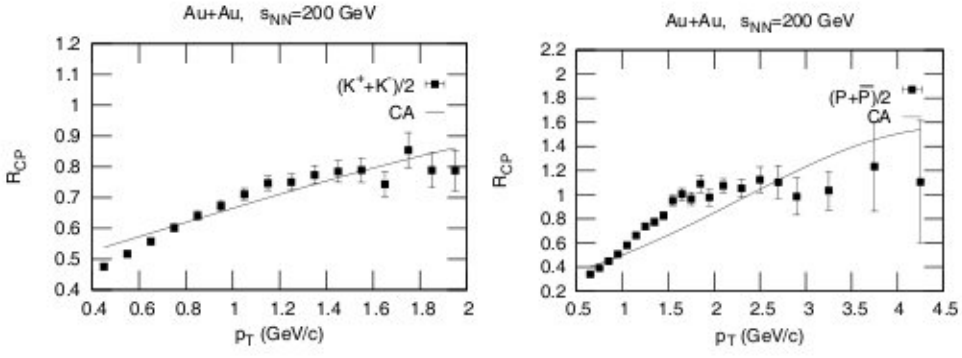

(c) (d)

Fig. 14 (*Continued*)

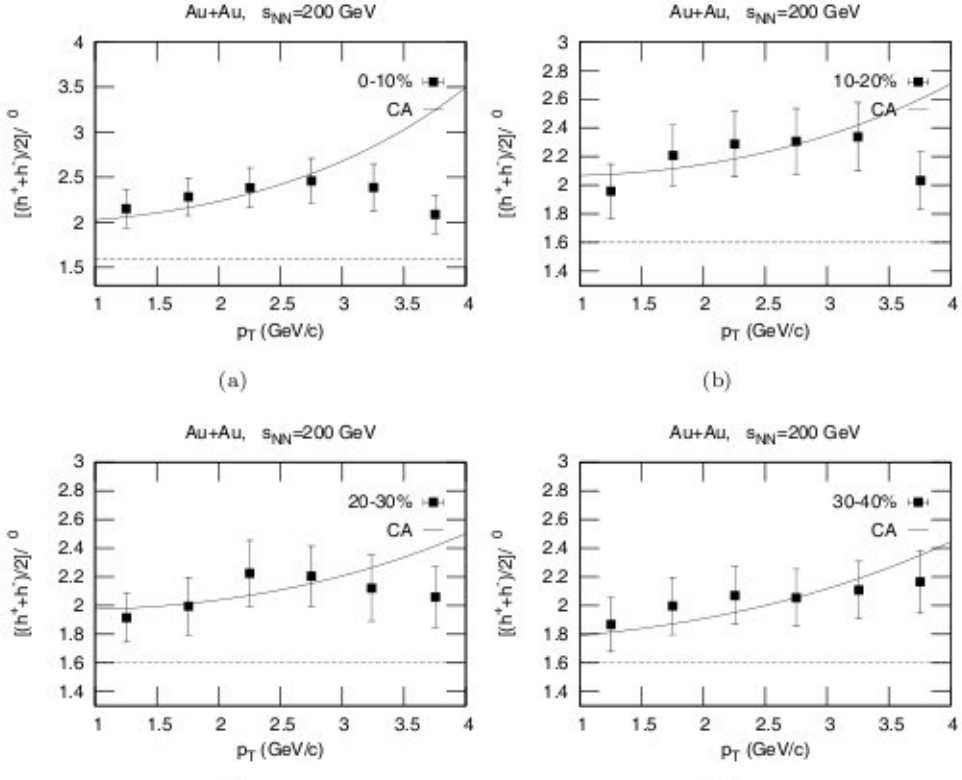

(a) (b)

(c) (d)

Fig. 15. The p_T-dependence of ratios of charged hadrons to neutral pions produced in AuAu collision at $\sqrt{s_{NN}} = 200$ GeV at different centralities. The various experimental data are taken from Ref. 7. The solid lines give the CA-based results. The dashed line at 1.6 is h/π ratio measured in $p + p$ and $e^+ + e^-$ collisions.

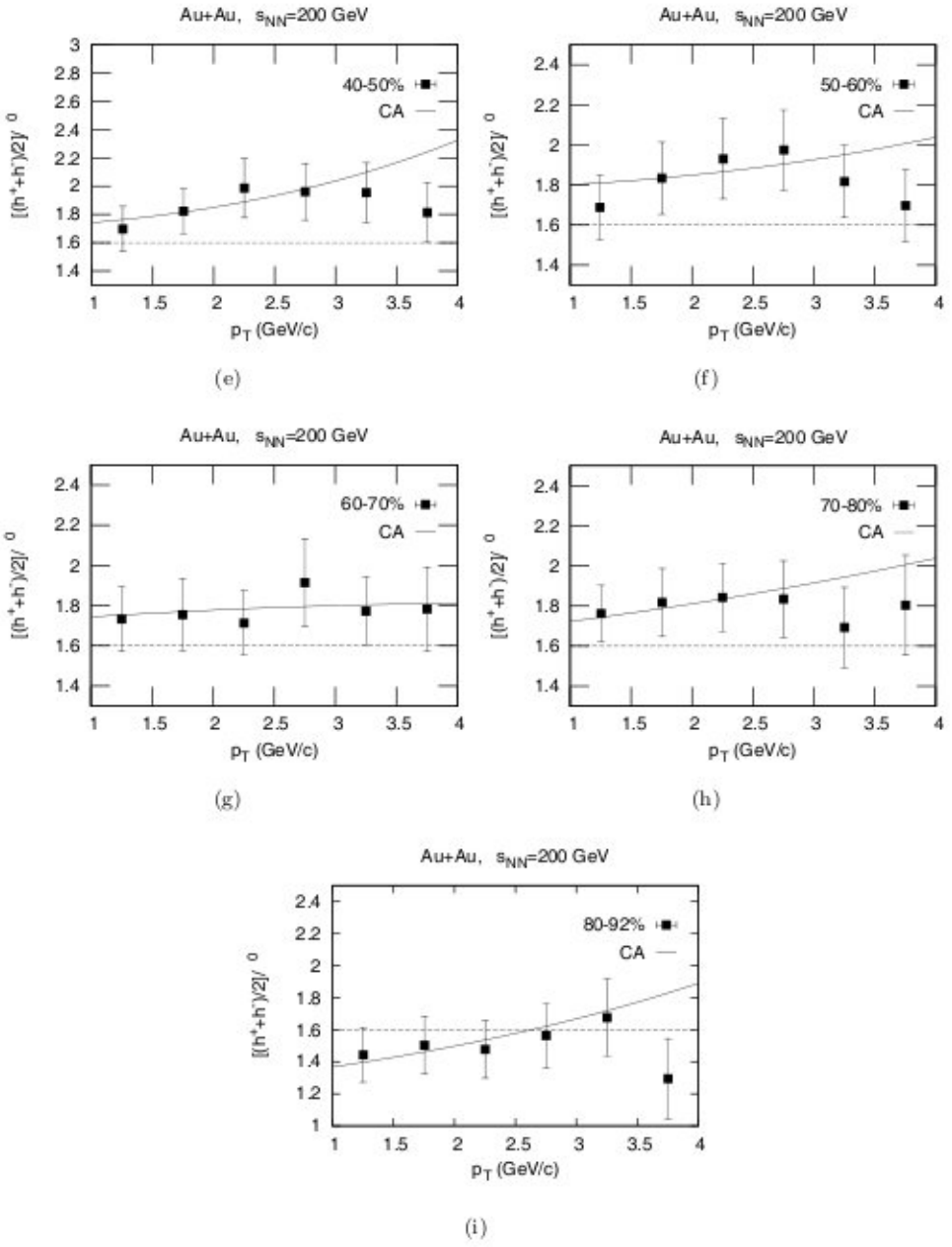

Fig. 15 (*Continued*)

Let us also make some points very clear and categorical. First, we strongly believe that even the most refined and reliable data sets obtained from just a single set of nuclear collisions at two or three different energies cannot and do not lead to any conclusive evidence either in support of or in opposition to certain preconceived

notions. Second, it is generally agreed that the data on D Au collisions were collected with the specific purpose of testing the so-called "jet-quenching" hypothesis. But, one must admit that, under such constraints, it might be difficult for the experimentalists to search for the physical reality in an unbiased and value-neutral way, leading to the confirmation of any set of results or observations, whatsoever.

Finally, the question is: what do we learn from this basically phenomenological study? This does essentially reflect that none of the theories projected so far could be considered to be either convincing or sufficient for our understanding of the physical realities connected with the gamut of observations made in both gold–gold and deuteron–gold collisions at very high energies, because even a sheer parametrization of data in a successful way, as is done here, could take care of all or most of the predicted/measured features on the relevant observables. Besides, even within the precincts of the standard model the explanation for the totality of the observed facts is nowhere possible. Rather, the points of views are too varied and the understanding so far, if any, is only partial, limited and fragmented. In fact, this would be somewhat clear and evident from an honest reiteration made by D. Enterria[1] "the whole set of experimental data puts strong constraints on the different proposed physical explanations for the underlying QCD medium produced in heavy ion collisions at RHIC and at LHC energies." Against this background, the present work assumes a much higher degree of importance and significance.

Acknowledgments

The authors would like to express their thankful gratitude to the learned referee for pointing out a gross information-related error contained in the previous draft of the manuscript of this work. It is also a pleasure to thank the honorable editor for his very permissive and positive roles in discharging the editorial tasks.

References

1. D. Enterria, nucl-ex/0309015 v-2.
2. B. De and S. Bhattacharyya, submitted to *Int. J. Mod. Phys. E.*
3. PHENIX Collab. (S. S. Adler *et al.*), *Phys. Rev. Lett.* **91**, 072303 (2003).
4. STAR Collab. (J. Adams *et al.*), *Phys. Rev. Lett.* **91**, 072304 (2003).
5. PHOBOS Collab. (B. B. Back *et al.*), *Phys. Rev. Lett.* **91**, 072302 (2003).
6. BRAHMS Collab. (I. Arsene *et al.*), *Phys. Rev. Lett.* **91**, 072305 (2003).
7. PHENIX Collab. (S. S. Adler *et al.*), *Phys. Rev. C* **69**, 034910 (2004).
8. PHENIX Collab. (S. S. Adler *et al.*), *Phys. Rev. C* **91**, 072301 (2004).
9. B. De, S. Bhattacharyya and P. Guptaroy, *J. Phys. G* **28**, 2963 (2002).
10. B. De and S. Bhattacharyya, *Int. J. Mod. Phys. A* **19**, 3225 (2004).
11. B. De and S. Bhattacharyya, *Mod. Phys. Lett. A* **18**, 1383 (2003).
12. B. De and S. Bhattacharyya, *Eur. Phys. J. A* **19**, 237 (2004).
13. UA1 Collab. (G. Arnison *et al.*), *Phys. Lett. B* **118**, 167 (1982).
14. UA1 Collab. (G. Bocqet *et al.*), *Phys. Lett. B* **366**, 434 (1996).
15. WA80 Collab. (R. Albrecht *et al.*), *Eur. Phys. J. C* **5**, 255 (1998).

16. R. Hagedorn, *Riv. Nuovo Cimento* **6**, 46 (1983); R. Hagedorn, CERN-TH.3684, 1983.
17. T. Peitzmann, *Phys. Lett. B* **450**, 7 (1999).
18. M. Giffon *et al.*, *Lett. Nuovo Cimento* **26**, 230 (1979); M. Giffon and E. Predazzi, *Z. Phys. C* **1**, 87 (1979).
19. BRAHMS Collab. (I. Arsene *et al.*), nucl-ex/0403005.
20. PHENIX Collab. (J. Jia), *Nucl. Phys. A* **715**, 769 (2003), http://www.phenix.bnl.gov/WWW/publish/jjia/qm02.pdf.
21. PHENIX Collab. (S. S. Adler *et al.*), *J. Phys. G* **30**, S335 (2004).